JOURNAL OF AGRICULTURAL AND FOOD CHEMISTRY

Reinvestigation of the Chemical Structure of Bitter-Tasting Quinizolate and Homoquinizolate and Studies on Their Maillard-Type Formation Pathways Using Suitable ^{13}C-Labeling Experiments

OLIVER FRANK AND THOMAS HOFMANN*

Deutsche Forschungsanstalt für Lebensmittelchemie, Lichtenbergstrasse 4, D-85748 Garching, Germany

Very recently, application of taste dilution analysis to heated xylose/alanine solutions led to the isolation of two bitter-tasting compounds exhibiting extraordinarily low detection thresholds of 0.00025 and 0.001 mmol/kg of water, respectively. On the basis of LC-MS and NMR spectroscopy, the structures of these compounds, named quinizolate and homoquinizolate, were proposed as 1-oxo-1*H*,4*H*-quinolizinium-7-olates. Since recent experiments in our laboratory shed some doubt on the entire correctness of their structures, labeling experiments with mixtures of multiply ^{13}C-labeled and nonlabeled pentoses were performed to follow the joint transfer of several ^{13}C atoms en bloc into the bitter compounds by LC-MS and NMR isotopomer diagnosis. The site-specific visualization of the mosaics assembled from ^{13}C-labeled and ^{12}C-labeled carbon modules in both bitter compounds demonstrated the structures of quinizolate and homoquinizolate to be the previously unknown (2*E*)-7-(2-furylmethyl)-2-(2-furylmethylidene)-3-(hydroxymethyl)- and (2*E*)-7-(2-furylmethyl)-2-(2-furylmethylidene)-3,8-bis(hydroxymethyl)-1-oxo-2,3-dihydro-1*H*-indolizinium-6-olate.

KEYWORDS: Quinizolate; homoquinizolate; taste compounds; bitter taste; ^{13}C-labeling; Maillard reaction; carbon module labeling; bond labeling; CAMOLA

INTRODUCTION

Besides the typical brown color and the aroma, the unique taste of thermally processed foods originates mainly from a complex network of reactions between reducing carbohydrates and amino compounds, collectively referred to as the Maillard reaction. The quality, intensity, and persistence of the bitter taste developing during, for example, baking or roasting processes strongly determines the consumer acceptance of roasted coffee, bread crust, roasted meat, sugar caramel, or kiln-dried malt. To further improve the sensory quality of processed foods by controlling the taste development more efficiently, first, a better understanding of the chemical structures of the most intense taste compounds is required, and then, knowledge of their precursors and formation pathways is a necessary prerequisite.

Whereas detailed information on the chemical nature and formation of flavorants is available on the volatile odor-active compounds in processed foods such as bread crust (*1*), heated beef (*2*), malt (*3*), and chocolate (*4*), only a few scientific papers are available on the thermal generation of taste compounds (*5*−*9*). To elucidate the key tastants formed during thermal food processing from Maillard-type reactions, we recently developed the so-called taste dilution analysis (TDA), which is based on the determination of the taste threshold of reaction products in serial dilutions of HPLC fractions (*10*, *11*). Application of this novel bioassay led to the detection of intense bitter-tasting compounds in heated aqueous solutions of xylose and L-alanine. On the basis of LC-MS and NMR experiments, the structure of the most intense bitter tastant, named quinizolate, was proposed as 3-(2-furyl)-8-[(2-furyl)methyl]-4-hydroxymethyl-1-oxo-1*H*,4*H*-quinolizinium-7-olate (**1a** in **Figure 1**) (*10*). This novel compound, exhibiting an intense bitter taste at an extraordinarily low detection threshold of 0.00025 mmol/kg of water, is one of the most potent bitter compounds reported so far (*10*). In addition, the structure of an homologous compound, recently isolated from a heated xylose/L-alanine solution, exhibited an additional hydroxymethyl group and was proposed as 3-(2-furyl)-8-[(2-furyl)methyl]-4,5-bis(hydroxy-methyl)-1-oxo-1*H*,4*H*-quinolizinium-7-olate (**1b** in **Figure 1**) (*12*). This compound, named homoquinizolate, imparted a strong bitter taste at a detection threshold of 0.001 mmol/kg of water, which is 4-fold above the threshold found for quinizolate but below the threshold of caffeine by a factor of 500 (unpublished results). Recent experiments in our laboratory, however, shed some doubt on the correctness of the chemical structures of quinizolate and homoquinizolate.

In addition to the chemical structures, the precursors and the formation pathways leading to these enormously bitter-tasting

* To whom correspondence should be adressed. Phone: +49-89-289 14170. Fax: +49-89-289 14183. E-mail: thomas.hofmann@lrz.tu-muenchen.de.

10.1021/jf020473k CCC: $22.00
Published on Web 09/07/2002

Table 1. Assignment of ^{1}H NMR Signals (400 MHz, DMSO-d_6) of Quinizolate and Homoquinizolate

H at relevant C atom[a]	δ (ppm)[b] quinizolate	δ (ppm)[b] homoquinizolate	I[c]	mult[c]	J (Hz)[c]	homonuclear ^{1}H,^{1}H connectivity[d]
H–C(15)	3.92	4.10	2	s		
H_a–C(5)	4.06	4.06	1	m	11.75	H_b–C(5), HO–C(5), H–C(4)
H–C(9′)		4.12	2	dd	5.29	HO–C(9′)
H_b–C(5)	4.23	4.23	1	m	11.75	H_a–C(5), HO–C(5), H–C(4)
HO–C(9′)		4.99	1	t	5.29	H–C(9′)
HO–C(5)	5.26	5.33	1	t	5.44	H_a–C(5), H_b–C(5)
H–C(4)	5.89	5.89	1	dd	1.52	H–C(10), H_a–C(5), H_b–C(5)
H–C(17)	6.26	5.98	1	d	3.5	H–C(18), H–C(19)
H–C(18)	6.43	6.30	1	dd	3.5, 1.8	H–C(17), H–C(19)
H–C(13)	6.78	6.78	1	dd	3.5, 1.8	H–C(12), H–C(14)
H–C(12)	7.19	7.19	1	d	3.5	H–C(13), H–C(14)
H–C(10)	7.34	7.34	1	d	1.52	H–C(4)
H–C(9)	7.45		1	s		
H–C(19)	7.60	7.47	1	d	1.8	H–C(17), H–C(18)
H–C(6)	7.96	7.96	1	s		
H–C(14)	8.05	8.04	1	d	1.8	H–C(12), H–C(13)

[a] Arbitrary numbering of carbon atoms refers to structures **1a/2a** for quinizolate and to **1b/2b** for homoquinizolate (**Figure 1**). [b] The ^{1}H chemical shifts are given in relation to DMSO-d_6. [c] Determined from 1D spectrum. [d] Homonuclear ^{1}H,^{1}H connectivities observed by a DQF–COSY experiment.

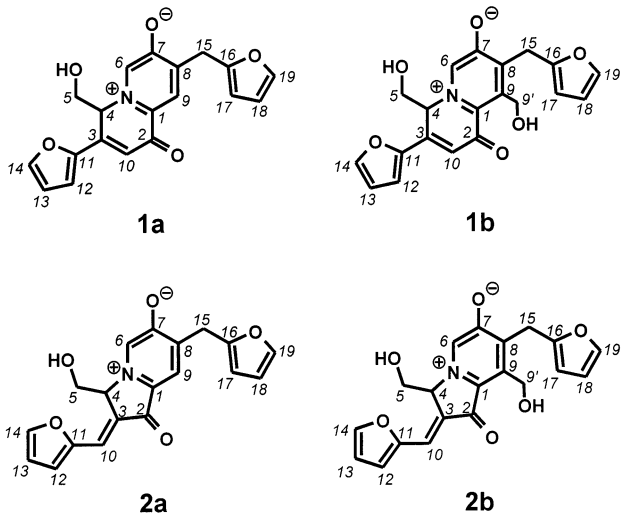

Figure 1. Chemical structures discussed for quinizolate (**1a**, **2a**) and homoquinizolate (**1b**, **2b**). Structures **1a/1b** were recently suggested on the basis of 1D and 2D NMR data only (*10*, *12*); structures **2a**/**2b** were unequivocally determined by ^{13}C-labeling experiments using LC-MS and NMR spectroscopic isotopomer diagosis.

compounds are still unclear. To clarify their precursors and to propose reaction pathways by which the carbohydrate is converted into the tastants in the course of Maillard-type reactions, a promising approach might be to react mixtures of various amino acids and carbohydrates as well as certain Maillard intermediates, which are most likely involved in tastant formation, and to determine the effectivity of these potential precursors in generating quinizolate and homoquinizolate by means of quantitative measurements. This concept was successfully used to identify the precursors of several key food odorants, such as the coffee character impact odorant 2-furfurylthiol (*13*) and the roasty-smelling 2-acetyl-2-thiazoline (*14*), as well as those of intense Maillard-type chromophores, such as (1*R*,8a*R*)- and (1*S*,8a*R*)-4-(2-furyl)-7-[(2-furyl)methylidene]-2-hydroxy-2*H*,7*H*,8a*H*-pyrano[2,3-*b*]pyran-3-one (*15*) and (*Z*)-2-[(2-furyl)methylidene]-5,6-di(2-furyl)-6*H*-pyran-3-one (*16*). It is then a necessary further step to propose mechanisms by which these precursors might be converted into the tastants. ^{13}C-Labeling experiments are believed to be most promising to follow how the carbon skeletons of certain carbohydrate degradation products are converted into the compound under investigation (*15*−*18*).

The objectives of the present studies were, therefore, to reinvestigate the chemical structures of quinizolate and homoquinizolate, to determine the precursor effectivity of carbohydrates, carbohydrate degradation products, and amino acids, and to propose reaction pathways governing their formation by application of carefully planned ^{13}C-labeling experiments.

MATERIALS AND METHODS

Chemicals. The following compounds were obtained commercially: D-xylose, D-ribose, D-glucose, D-fructose, glycine, L-alanine, L-valine, L-leucine, L-proline, furan-2-aldehyde, acetaldehyde, acetic acid, glycolaldehyde, glyoxal, glyoxylic acid, and oxalic acid (Aldrich, Steinheim, Germany); [$^{13}C_5$]-D-ribose (Omicron Biochemicals, South Bend, IN). Furan-2-aldehyde was freshly distilled at 30 °C under high vacuum prior to use. Solvents were HPLC-grade (Aldrich, Steinheim, Germany). The bitter compounds quinizolate (*10*) and homoquinizolate (*12*) were isolated from a heated xylose/alanine solution following the procedures reported recently, and their identity and a purity of >99% were checked by NMR spectroscopy (**Tables 1** and **2**).

Quantitation of Quinizolate and Homoquinizolate in Heated Maillard Model Mixtures. To study the influence of the carbohydrate moiety on tastant formation, binary solutions of L-alanine (38 mmol) and the carbohydrates xylose, ribose, glucose, and fructose (150 mmol each), respectively, were refluxed in phosphate buffer (100 mL, 0.1 mol/L, pH 5.0) for 3 h. For the furan-2-aldehyde-spiking experiment, the corresponding xylose/alanine mixture was refluxed for 2 h in the absence or in the presence of furan-2-aldehyde (38 mmol). After cooling, the pH of these solutions as well as the reaction mixtures detailed in the figure legends was adjusted to 4.5 by adding aqueous hydrochloric acid (0.1 mol/L), the aqueous solutions were extracted with ethyl acetate (5 × 20 mL), and the combined organic layers were dried over Na_2SO_4 and then distilled under high vacuum (0.04 mbar) at 35 °C. The nonvolatile residue of each extraction was dissolved in a minimum amount of ethyl acetate and was applied onto the top of a water-cooled glass column (450 mm × 35 mm) filled with silica gel 60 (200 g) (Merck, Darmstadt, Germany), which was preconditioned with toluene/ethyl acetate (80/20 v/v). Chromatography was performed using toluene/ethyl acetate (80/20 v/v, 300 mL, fraction A), followed by toluene/ethyl acetate (50/50 v/v, 300 mL, fraction B), ethyl acetate (300 mL, fraction C), ethyl acetate/methanol (90/10 v/v, 300 mL, fraction D), ethyl acetate/methanol (80/20 v/v, 300 mL, fraction E), and ethyl acetate/methanol (50/50 v/v, 300 mL, fraction F). Fraction E, containing both tastants, was collected and freed from solvent in vacuo at 25 °C. The residue was taken up in methanol (5 mL), and

Table 2. Assignment of ^{13}C NMR Signals (500 MHz, DMSO-d_6) of Quinizolate and Homoquinizolate

H at relevant C atom[a]	δ (ppm)[b]			heteronuclear $^1H,^{13}C$ connectivity[d]	
	quinizolate	homoquinizolate	DEPT[c]	via $^1J_{C,H}$	via $^{2,3}J_{C,H}$
C(15)	27.7	25.5	CH_2	H–C(15)	
C(9′)		54.0	CH_2	H–C(9′)	HO–C(9)
C(5)	62.0	62.2	CH_2	H–C(5)	HO–C(5), H–C(4)
C(4)	67.9	67.6	CH	H–C(4)	H–C(5), H–C(10), H–C(6)
C(17)	107.3	105.7	CH	H–C(17)	H–C(18), H–C(19)
C(18)	110.6	110.3	CH	H–C(18)	H–C(17), H–C(19)
C(13)	113.4	113.4	CH	H–C(13)	H–C(12), H–C(14)
C(10)	117.8	117.6	CH	H–C(10)	
C(12)	119.7	119.5	CH	H–C(12)	H–C(13), H–C(14)
C(9)	120.4	138.7	CH/C	H–C(9)	H–C(9′), H–C(15)
C(1)	125.7	123.7	C		H–C(6), H–C(9)
C(3)	126.7	127.2	C		H–C(4), H–C(10)
C(6)	129.9	130.4	CH	H–C(6)	
C(19)	142.1	141.2	CH	H–C(19)	H–C(17), H–C(18)
C(8)	142.4	140.5	C		H–C(6), H–C(9), H–C(15)
C(14)	147.5	147.4	CH	H–C(14)	H–C(12), H–C(13)
C(11)	150.0	150.0	C		H–C(10), H–C(12), H–C(13), H–C(14)
C(16)	151.9	152.5	C		H–C(17), H–C(18), H–C(19)
C(7)	171.0	170.7	C		H–C(6), H–C(9), H–C(15)
C(2)	180.0	180.6	C		H–C(10), H–C(9)

[a] Arbitrary numbering of carbon atoms refers to structures **1a/2a** for quinizolate and **1b/2b** for homoquinizolate (**Figure 1**). [b] The ^{13}C chemical shifts are given in relation to DMSO-d_6. [c] DEPT-135 spectroscopy. [d] Assignments based on HSQC ($^1J_{C,H}$) and HMBC ($^{2,3}J_{C,H}$) experiments.

after membrane filtration, the solution was analyzed by analytical RP-HPLC. Identification of the target compounds was performed by comparison of the LC-MS and the UV/vis spectra as well as the retention times with those obtained for the pure reference compounds. Quantitation of quinizolate and homoquinizolate was performed by comparing the peak areas obtained at $\lambda = 412$ nm with those of defined standard solutions of each reference compound in methanol. The results given in **Figures 2** and **6**−**8** are the mean of triplicates.

"Carbon Module Labeling" (CAMOLA) Experiment. A solution of D-ribose (1.6 mmol), [$^{13}C_5$]D-ribose (1.6 mmol), and L-alanine (1.6 mmol) in phosphate buffer (10 mL, 1 mmol/L, pH 5.0) was refluxed for 20 min, and then furan-2-aldehyde (5.0 mmol) was added and heating was continued for another 60 min. After the reaction mixture was cooled to room temperature, the pH was adjusted to 4.5, and the aqueous solution was extracted with ethyl acetate (5 × 10 mL). The combined organic layers were dried over Na_2SO_4, concentrated to about 1 mL, and then fractionated by flash chromatography using silica gel (200 g, Silica Gel 60, 6% water, Merck, Darmstadt, Germany) as the stationary phase. After application of the crude material onto the top of the water-cooled glass column (30 mm × 350 mm) conditioned with toluene/ethyl acetate (50/50 v/v), chromatography was performed using toluene/ethyl acetate (50/50 v/v, fraction A), followed by ethyl acetate (250 mL, fraction B), ethyl acetate/methanol (80/20 v/v, 250 mL, fraction C), and ethyl acetate/methanol (50/50 v/v, 250 mL, fraction D). Fraction C, containing the isotopomers of quinizolate and homoquinizolate, was collected, freed from solvent in vacuo, and taken up in methanol (1 mL). Comparative HPLC-MS analysis of pure reference solutions of both tastants and of the solution obtained from fraction C revealed the isotopomeric patterns of the quasi-molecular ions ([M + 1]$^+$) of nonlabeled and labeled quinizolate and homoquinizolate, respectively, illustrated in **Figures 2** and **3**.

"Carbon Bond" Labeling. A solution of D-ribose (63.3 mmol), [$^{13}C_5$]D-ribose (3.3 mmol), and l-alanine (33.3 mmol) in phosphate buffer (45 mL, 1 mmol/L, pH 3.0) was refluxed for 20 min, and then furan-2-aldehyde (25.0 mmol) was added and heating was continued for another 3 h. After being cooled to room temperature, the aqueous solution was extracted with ethyl acetate (5 × 25 mL). The combined organic layers were dried over Na_2SO_4, filtrated, and then freed from solvent in vacuo. The yellow residue was dissolved in methanol (2 mL), membrane filtered, and then fractionated by semipreparative RP-HPLC. Monitoring the effluent at $\lambda = 412$ nm, two major peaks containing the target compounds were collected and freeze-dried twice. Quinizolate (1.9 mg) and homoquinizolate (1.0 mg) were obtained in a purity of >99% and were taken up in DMSO-d_6 for ^{13}C NMR

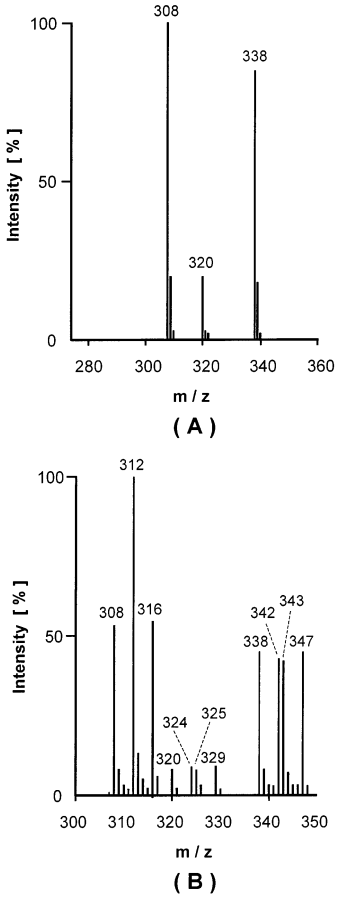

Figure 2. LC-MS spectra of isotopomers of quinizolate formed from (A) natural abundance [^{13}C]ribose in the presence of L-alanine and (B) a 1:1 mixture of natural abundance [^{13}C]ribose and [$^{13}C_5$]ribose in the presence of L-alanine and furan-2-aldehyde.

experiments (**Table 3**). As an example, the coupling patterns of the ^{13}C signals of labeled quinizolate are illustrated in **Figure 4**.

High-Performance Liquid Chromatography (HPLC). The HPLC apparatus (Kontron, Eching, Germany) consisted of two pumps (type 422), a gradient mixer (M 800), a Rheodyne injector (100 μL loop),

Table 3. Assignment of ^{13}C NMR Signals (500 MHz, DMSO-d_6) in 5% ^{13}C-Enriched Quinizolate and Homoquinizolate

H at relevant C atom[a]	δ (ppm)[b]			homonuclear $^{13}C,^{13}C$ connectivities via $^{1,2,3}J_{C,C}$ (Hz) of[d]	
	quinizolate	homoquinizolate	mult[c]	quinizolate	homoquinizolate
C(15)	27.7	25.5	s		
C(9′)		54.0	d		C(9) [44.5]
C(5)	62.0	62.2	d	C(4) [36.0]	C(4) [36.7]
C(4)	67.9	67.6	ddd	C(2) [3.1], C(3) [47.8], C(5) [36.0]	C(2) [3.1], C(3) [49.5], C(5) [36.7]
C(17)	107.3	105.7	s		
C(18)	110.6	110.3	s		
C(13)	113.4	113.4	s		
C(10)	117.8	117.6	s		
C(12)	119.7	119.5	s		
C(9)	120.4	138.7	dd/ddd	C(7) [2.6], C(8) [61.0]	C(7) [2.9], C(8) [60.4], C(9′) [44.5]
C(1)	125.7	123.7	dd	C(2) [67.4], C(3) [17.2]	C(2) [67.9], C(3) [17.0]
C(3)	126.7	127.2	ddd	C(1) [17.2], C(2) [54.0], C(4) [47.8]	C(1) [17.0], C(2) [52.6], C(4) [49.5]
C(6)	129.9	130.4	dd	C(7) [62.4], C(8) [15.5]	C(7) [61.5], C(8) [14.6]
C(19)	142.1	141.2	s		
C(8)	142.4	140.5	ddd	C(6) [15.5], C(7) [55.3], C(9) [61.0]	C(6) [14.6], C(7) [56.0], C(9) [60.4]
C(14)	147.5	147.4	s		
C(11)	150.0	150.0	s		
C(16)	151.9	152.5	s		
C(7)	171.0	170.7	ddd	C(6) [62.4], C(8) [55.3], C(9) [2.6]	C(6) [61.5], C(8) [56.0], C(9) [2.9]
C(2)	180.0	180.6	ddd	C(1) [67.4], C(3) [54.0], C(4) [3.1]	C(1) [67.9], C(3) [52.6], C(4) [3.1]

[a] Arbitrary numbering of carbon atoms refers to structure **2a** (quinizolate) and to **2b** (homoquinizolate) in **Figure 1**. [b] The ^{13}C chemical shifts are given in relation to DMSO-d_6. [c] Multiplicity was taken from ^{13}C spectrum. [d] Assignments based on a ^{13}C ($^{1,2,3}J$) experiment.

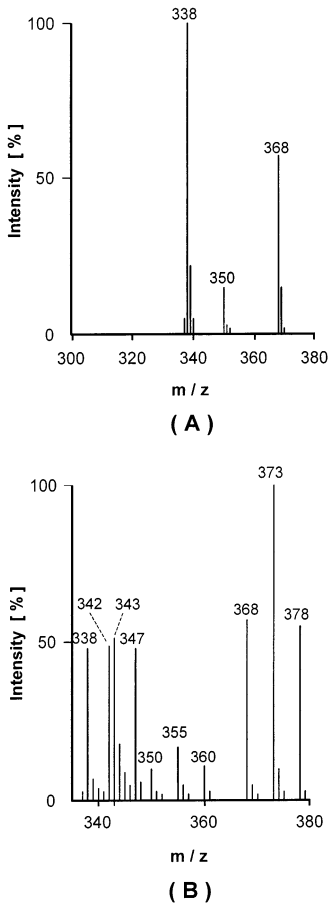

Figure 3. LC-MS spectra of isotopomers of homoquinizolate formed from (A) natural abundance [^{13}C]ribose and L-alanine and (B) a 1:1 mixture of natural abundance [^{13}C]ribose and [$^{13}C_5$]ribose in the presence of L-alanine and furan-2-aldehyde.

and a diode array detector (DAD type 540), monitoring the effluent in a wavelength range between 220 and 500 nm. Separations were performed on a stainless steel column packed with RP-18 (ODS-Hypersil, 5 μm) (Shandon, Frankfurt, Germany) either on an analytical (4.6 mm × 250 mm, 0.8 mL/min) or a semipreparative scale (10 mm × 250 mm, 1.6 mL/min). After injection of the sample (20−100 μL), analysis was performed using a gradient starting with a mixture (80/20 v/v) of aqueous ammonium formate (10 mmol/L, pH 3.5) and methanol and increasing the methanol content to 100% within 40 min.

Liquid Chromatography−Mass Spectrometry (LC-MS). An analytical HPLC column (Nucleosil 100-5C18, 4.6 × 250 mm) (Macherey and Nagel, Dürren, Germany) was coupled to an LCQ-MS (Finnigan MAT GmbH, Bremen, Germany) using atmospheric pressure chemical ionization (APCI). After injection of the sample (20−100 μL), analysis was performed using a gradient starting with a mixture (80/20 v/v) of aqueous ammonium formate (10 mmol/L, pH 3.5) and methanol and increasing the methanol content to 100% within 40 min. For LC-MS/MS measurements, the sample (10 μg/mL) was dissolved in water/methanol (10/20 v/v) and then applied to the MS by using the loop injection technique (injection speed, 10 μL/min). For each fragmentation step, one ion was separated by means of an ion trap and then fragmented separately.

Nuclear Magnetic Resonance Spectroscopy (NMR). 1D and 2D NMR experiments were performed on a Bruker AMX-400 (^1H frequency, 400.13 MHz) and a Bruker-Avance-500 spectrometer (^{13}C frequency, 125.70 MHz) (Bruker, Rheinstetten, Germany). Chemical shifts were measured from residual DMSO-d_5 (2.49 ppm) in the proton spectra and from the carbon signal of DMSO-d_6 (39.5 ppm) in the carbon spectra.

RESULTS AND DISCUSSION

The structures **1a** and **1b** recently proposed for the intensely bitter compounds quinizolate and homoquinizolate are shown in **Figure 1**. It seems obvious from these structures that both the furan rings C(11)−C(14) and C(16)−C(19) in **1a**/**1b** correspond to two molecules of furan-2-aldehyde derived from pentose degradation. To prove the key role of this carbohydrate intermediate as one of the precursors, furan-2-aldehyde was added to an aqueous solution of xylose and L-alanine prior to thermal treatment, and the amounts of both tastants were quantified after heating. In comparison, a control experiment was performed, in which the xylose/alanine mixture was heated in the absence of furan-2-aldehyde. The yields of quinizolate and homoquinizolate increased from 5.1 and 2.3 μmol, respectively, by a factor of about 6 to 31.1 and 15.0 μmol when the

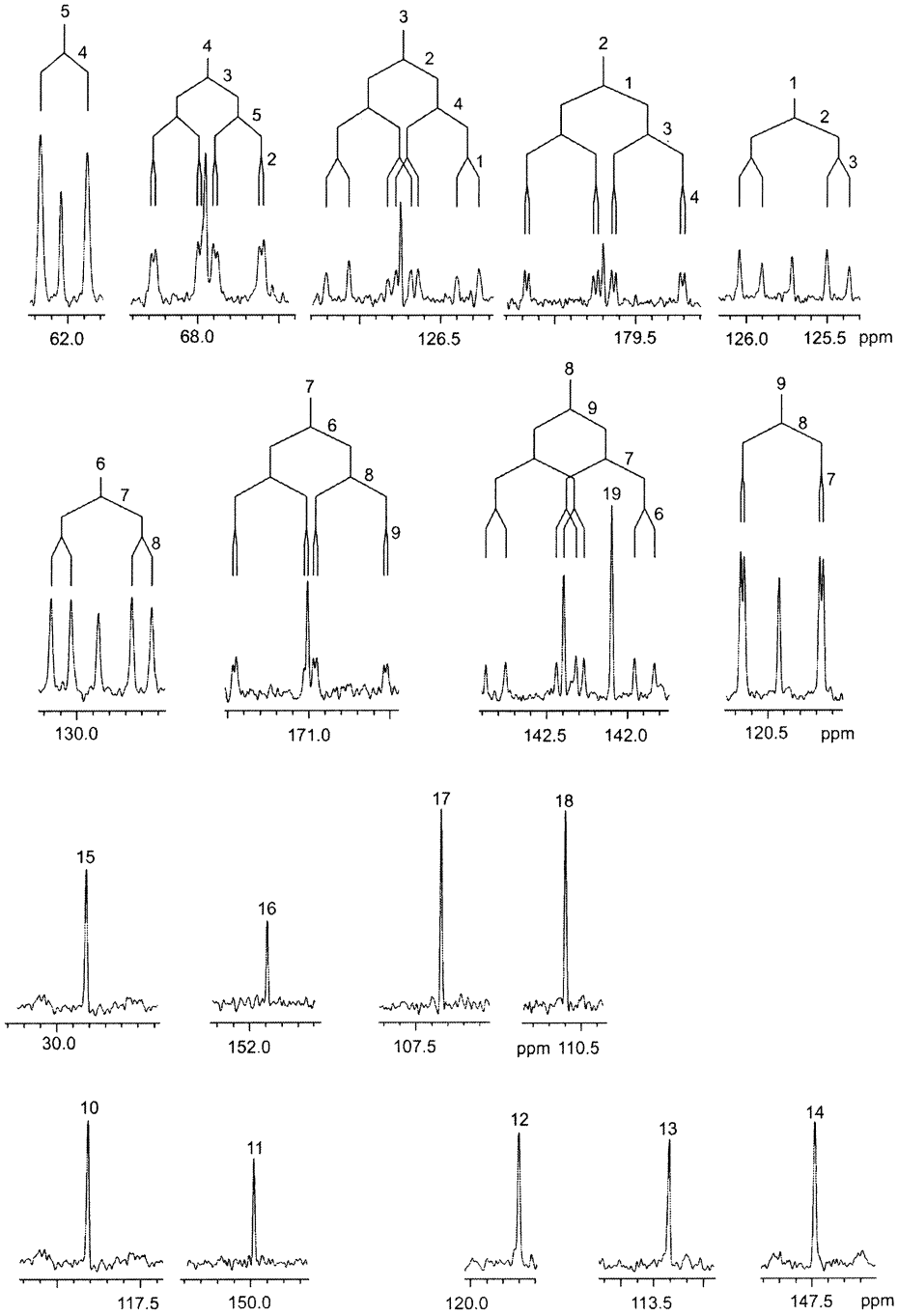

Figure 4. Excerpts of the ^{13}C NMR spectrum of quinizolate isotopomers isolated from a heated ribose/alanine/furan-2-aldehyde mixture containing 5% [$^{13}C_6$]ribose (arbitrary numbering given above the center signal of the carbon atoms as well as the couplings between the centered carbon atom and neighboring atoms refer to structure **2a** in **Figure 1**).

pentose and L-alanine were reacted in the presence of furan-2-aldehyde. These data clearly demonstrate that furan-2-aldehyde acts as an effective precursor and is incorporated into the structures of both pyridinium betains, thus confirming its proposed key role in the formation of quinizolate and homoquinizolate.

Assuming that the intact C_5-carbon skeleton of furan-2-aldehyde is incorporated without any fragmentation into the taste compounds, it has to be accepted that, besides both of the furan rings, the neigboring carbon atoms C(3) and C(15) in structure **1a**/**1b** (**Figure 1**) also originate from furan-2-aldehyde. This indicates that the furan-2-aldehyde-derived carbon atom C(3) in **1a**/**1b** would interrupt the contiguity of the carbon skeleton in the 1-oxo-1*H*,4*H*-quinolizinium-7-olate ring system, which is most likely formed via other carbohydrate intermediates, thus implying that the hydroxyethylidene group C(4)−C(5) connected via C(4) with the nitrogen atom and the furan-2-aldehyde-derived C(3) of the (2-furyl)methine system might originate from a C_2-carbohydrate fragment.

To answer the question of whether the carbon moiety C(4)−C(5) in **1a** and **1b** stems from a C_2-carbohydrate fragment, the xylose/L-alanine mixture was heated in the presence of several exogeneously added potential C_2-carbohydrate fragments, namely acetaldehyde, acetic acid, glycolaldehyde, glyoxal, glyoxylic acid, and oxalic acid. Neither varying the type of the C_2-fragment nor changing the reactant concentrations or the reaction conditions led to a favored production of quinizolate and homoquinizolate (data not shown). These results, therefore,

indicate that the C(4)−C(5) moiety in the tastants most likely does not originate from a C_2-fragment. Taking into consideration that, on one hand, the carbon atom C(3) in **1a**/**1b**, supposed to stem from the carbonyl carbon of furan-2-aldehyde, interrupts the carbon skeleton in the lower pyridone ring into a C(1)−C(2)−C(10) and a C(4)−C(5) fragment, and, on the other hand, any exogeneously added C_2-fragment failed to operate as a precursor, it might be concluded that the chemical structures **1a** and **1b** for quinizolate and homoquinizolate are not entirely correct. Alternative structures, which would be consistent with these latest findings, might be created by shifting the endocyclic (2-furyl)methylidene group in the lower pyridone ring of **1a**/**1b** into an exocyclic position attached to a five-membered pyrrolinone ring, as illustrated in **2a** and **2b** (**Figure 1**).

Chemical Structures and Labeling Experiments. To reinvestigate the chemical structure of quinizolate and homoquinizolate, first, both taste compounds were again isolated from a heated aqueous solution of xylose and L-alanine on a semipreparative scale and purified by following the procedures reported recently (*10*, *12*). The assignment of the ^1H and ^{13}C NMR data of quinizolate and homoquinizolate, summarized in **Tables 1** and **2**, are in good agreement with structures **1a** and **1b** (**Figure 1**) proposed recently but do not allow differentiation from the alternative structures **2a** and **2b** (**Figure 1**). Heteronuclear multiple bond correlation (HMBC) experiments on both tastants revealed $^1H/^{13}C$ connectivity between the quaternary carbon atom C(3) and protons H−C(4) and H−C(10), between C(11) and H−C(10), and between the carbonyl atom C(2) and H−C(10). It is interesting to note that exactly the same heteronuclear correlations also support the structures **2a** and **2b**, differing from **1a**/**1b** in the exocyclic position of the (2-furyl)-methylidene group. In contrast to structures **1a** and **1b**, in the alternative structures **2a** and **2b**, fully reflecting the entire set of NMR data as well, the contiguity of the carbon skeleton C(1)−C(5) in the lower ring system would not be interrupted by the former carbonyl group of the furan-2-aldehyde, and would therefore be well in line with the finding that the addition of any C_2-fragment did not result in accelerated tastant formation.

To further strengthen this hypothesis, the following studies were aimed at monitoring the flux of intact carbon skeletons from the pentose into quinizolate and homoquinizolate by means of carefully planned ^{13}C-labeling strategies. The use of universally labeled carbohydrates as precursors in Maillard reactions will give rise to universally labeled taste compounds, implying that individual carbon fragments involved in the formation of quinizolate and homoquinizolate cannot be visualized. In comparison to singly and site-specifically labeled carbohydrates, the advantage of using multiply ^{13}C-labeled precusors is that the joint transfer of several ^{13}C atoms en bloc into the target compounds confirms that the carbon skeleton has remained intact during the passage of this fragment through the Maillard reaction sequence. Determining the number of carbon atoms which can be transferred en bloc would afford rigorous constraints for the intermediary pathway through which this carbon module has been processed. Because quinizolate and homoquinizolate are ultimately derived from the complex pool of transient Maillard reaction intermediates such as furan-2-aldehyde, deoxyosones, etc., their labeling patterns must reflect the carbon skeletons of intermediates involved in their formation. To visualize the mosaics assembled from ^{13}C-labeled and ^{12}C-labeled carbon modules, the [$^{13}C_5$]carbohydrate has, therefore, to be diluted with natural ^{13}C abundance carbohydrate prior to the Maillard reaction. The number of carbon atoms present in these modules can then be easily monitored in the target compounds by means of sophisticated LC-MS techniques.

Using this concept, named the "carbon module labeling" (CAMOLA) experiment (manuscript in preparation), an equimolar mixture of natural ^{13}C abundance and [$^{13}C_5$]ribose was heated in the presence of L-alanine. An excess of nonlabeled furan-2-aldehyde was added to the mixture prior to the thermal treatment, aimed at channeling the labeled carbon modules exclusively into the 9 or 10 carbon atoms of quinizolate or homoquinizolate, respectively, which do not stem from furan-2-aldehyde, already identified as a precursor. After chromatographic pre-separation of the reaction mixture, the isotopomeric patterns of quinizolate and homoquinizolate were analyzed by HPLC-MS and compared to the mass spectra obtained in the corresponding nonlabeled experiment (**Figures 2** and **3**). The mass spectrum of natural ^{13}C abundance quinizolate is displayed in **Figure 2A**. In comparison, the mass spectrum of the tastant isolated from the labeling experiment is outlined in **Figure 2B**, showing a 1:1:1:1 ratio of the $[M + 1]^+$ ions of four isotopomers formed. Besides the $[M + 1]^+$ ion with *m*/*z* 338, corresponding to nonlabeled quinizolate, the $[M + 1]^+$ ion of the 9-fold-labeled isotopomer was detected with *m*/*z* 347, thus confirming that two molecules of furan-2-aldehyde are incorporated into the tastant. In addition to the nonlabeled and the 9-fold-labeled isotopomers, two additional isotopomers showing $[M + 1]^+$ ions with *m*/*z* 342 and 343, respectively, were detected (**Figure 2B**). These results clearly demonstrate the incorporation of four and five ^{13}C labels, respectively, into quinizolate, thus indicating that the nine carbon atoms under investigation originate from carbohydrate degradation products with C_4- and C_5-carbon skeletons. In addition, a loss of 18 amu, most likely corresponding to the cleavage of a molecule of water from these quasi-molecular ions, revealed a 1:1:1:1 pattern of isotopomers showing *m*/*z* 320, 324, 325, and 329, thus demonstrating that the labeled carbon atoms are still present in these fragments (**Figure 2B**). As confirmed by LC-MS/MS, the fragment ion with *m*/*z* 308 results from its mother ion at *m*/*z* 338 by the loss of 30 amu, most likely corresponding to the elimination of the hydroxymethyl group C(5) as formaldehyde. In addition, fragmentation of the $[M + 1]^+$ ion with *m*/*z* 347 revealed the daugther ion at *m*/*z* 316 by a loss of 31 amu, corresponding to the cleavage of a molecule of [^{13}C]formaldehyde (**Figure 2B**). It is most interesting to note that the base ion, showing *m*/*z* 312, is formed as the daughter ion by fragmentation of both the $[M + 1]^+$ ions, *m*/*z* 342 and 343. This indicated that the isotopomer with *m*/*z* 342, generated by a 4-fold-labeled and a 5-fold-nonlabeled intermediate, showed a loss of 30 amu, corresponding to the cleavage of formaldehyde from the nonlabeled hydroxymethyl group C(5), whereas in the isotopomer with *m*/*z* 343, containing a 5-fold-labeled and a 4-fold-nonlabeled carbon backbone, one molecule of labeled formaldehyde (loss of 31 amu) was cleaved from the ^{13}C-labeled hydroxymethyl group. On the basis of these data, it has to be concluded that the hydroxymethyl group C(5) is part of the C_5-fragment involved in formation of quinizolate, thus fitting well with structure **2a** (**Figure 1**), exhibiting the exocyclic (2-furyl)-methylidene group.

Comparison of the LC-MS spectrum of nonlabeled homoquinizolate (**Figure 3A**) with that obtained for the isotopomeric mixture isolated from the ^{13}C-labeling experiment (**Figure 3B**) elucidated the $[M + 1]^+$ ions with *m*/*z* 368, 373, and 378, in a ratio of about 1:2:1, corresponding to nonlabeled, 5-fold-labeled and 10-fold-labeled homoquinizolate. These data clearly indicate that two carbohydrate-derived C_5-intermediates are involved in

its formation (**Figure 3B**). The identical labeling pattern is reflected in the fragment ions *m*/*z* 350, 355, and 360, being consistent with the loss of a molecule of water from the quasi-molecular ions of these isotopomers (**Figure 3B**). As confirmed by LC-MS/MS, the fragment ions with *m*/*z* 338 and 347 resulted from their mother ions *m*/*z* 368 and 378 by the loss of 30 and 31 amu, respectively, corresponding to the elimination of a hydroxymethyl group as nonlabeled and ^{13}C-labeled formaldehyde, respectively. In addition, LC-MS/MS of the base ion *m*/*z* 373 revealed that both of the fragment ions, *m*/*z* 342 and 343, originate in a ratio of about 1:1 from 5-fold-labeled isotopomers. These results, as well as the high intensity of the base ion *m*/*z* 373, clearly indicated the existence of two 5-fold-labeled isotopomers of homoquinizolate, one of which bears an activated hydroxymethyl group in the nonlabeled part of the molecule (loss of 30 amu to give *m*/*z* 343), and the other as part of the 5-fold-labeled carbon skeleton liberating the fragment *m*/*z* 342 upon cleavage of a ^{13}C-labeled formaldehyde. These data correspond well with the structure **2b** in **Figure 1**.

Although this CAMOLA experiment provides the possibility to elucidate the number of carbon atoms present in the individual carbon modules involved in the formation of the target compound, the exact positions of these carbon modules in the mosaic pattern of the target molecule cannot be visualized, and the assignment of the label to a single atom position cannot be easily achieved. In contrast, ^{13}C NMR spectroscopy can unequivocally detect site-specifically the presence of the isotope, even in cases of low ^{13}C-labeling enrichment rates. The joint transfer of several ^{13}C atoms en bloc from a multiply ^{13}C-labeled precursor confirms that the bonds between the respective atoms have remained intact during its transformation. The site-specific visualization of intact carbon bonds by measuring the ^{13}C/^{13}C coupling constants using ^{13}C NMR spectroscopic diagnostics, named "bond labeling", has been successfully used as a powerful tool to elucidate biosynthetic pathways in plants and microorganisms (*18*).

To unequivocally confirm the structures **2a** and **2b** for quinizolate and homoquinizolate and to elucidate their formation pathways, this "bond-labeling" technique was performed by heating natural ^{13}C abundance ribose, which was diluted with 5.0% [$^{13}C_5$]ribose, in the presence of L-alanine in aqueous solution. To black-out the ^{13}C/^{13}C couplings in the furan-2-aldehyde-derived fragments of quinizolate and homoquinizolate, the mixture was spiked with natural ^{13}C abundance furan-2-aldehyde prior to thermal treatment. After solvent extraction, both target compounds were isolated and purified by semiperparative RP-HPLC and then analyzed by ^{1}H broad-band-decoupled ^{13}C NMR spectroscopy. The chemical shifts and multiplicity of the carbon atoms as well as the ^{13}C/^{13}C coupling constants obtained for quinizolate and homoquinizolate are summarized in **Table 3**. As an example, the ^{13}C/^{13}C coupling patterns measured for each carbon atom in quinizolate are displayed in **Figure 4**.

Due to their natural ^{13}C abundance, the 10 carbon atoms C(15)−C(19) and C(10)−C(14) were detected as singlets, thus confirming that the intact C_5-skeleton of the pentose dehydration product furan-2-aldehyde, which was added as the natural ^{13}C abundance compound, is incorporated into quinizolate without any fragmentation (**Figure 4**). In contrast, the carbon atom C(6), resonating at 129.9 ppm, showed intense ^{13}C satellites as a double-doublet with coupling contants of 62.4 and 15.5 Hz, corresponding to the ^{1}J coupling with C(7) and the ^{2}J coupling with C(8). For the neighboring carbon C(7), a strongly coupled signal pattern was observed at 171.0 ppm, showing coupling

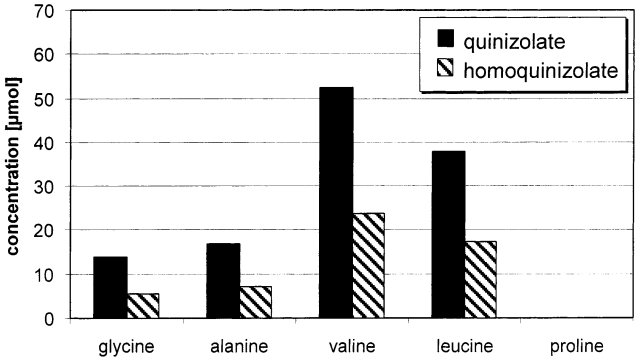

Figure 5. Influence of the amino acid moiety on the formation of quinizolate and homoquinizolate from xylose. Binary solutions of D-xylose (150 mmol) and amino acid (38 mmol each) in phosphate buffer (100 mL, 0.1 mol/L, pH 5.0) were heated under reflux for 3 h.

constants of 62.4, 55.3, and 2.6 Hz, corresponding to the coupling with the carbon atoms C(6), C(8), and C(9), respectively (**Figure 4**). For carbon atom C(8), resonating at 142.4 ppm, a complex coupling pattern was also observed (**Figure 4**). This quaternary carbon atom shows homonuclear coupling with C(9), C(7), and C(6) but does not show any homonuclear connectivity with C(15), thus confirming that C(15) is not ^{13}C-enriched. As depicted in **Table 3** and **Figure 4**, the carbon atom C(9) showed ^{13}C satellites as double-doublets with coupling constants of $^{1}J_{C(9)/C(8)} = 61.0$ and $^{2}J_{C(9)/C(7)} = 2.6$ Hz, but it showed no further coupling with the neighboring C(1). Taking all these data into account, it can be concluded that the carbon module C(6)−C(9) is shifted into the upper pyridinium ring of quinizolate as an intact C_4-fragment derived from the pentose.

To clarify the situation in the lower ring of quinizolate, the coupling patterns of C(1)−C(5) were investigated (**Table 3** and **Figure 4**). The hydroxymethyl group C(5), resonating at 62.0 ppm, showed only one homonuclear coupling to C(4), with a coupling constant of 36.0 Hz, thus indicating that the C(4) is, indeed, the only carbon atom directly connected with C(5) and confirming the finding that the C(5) is a terminal carbon atom in the second carbon module. In addition, for C(1), the coupling constants were found to be $^{1}J_{C(1)/C(2)} = 67.4$ and $^{2}J_{C(1)/C(3)} = 17.2$ Hz, but no further coupling to C(9) and C(10) was observable. These data confirmed the presence of the exocyclic (2-furyl)methylidene group in structure **2a** of quinizolate and, in addition, pointed out that the quaternary carbon atom C(1) is the other terminal atom in this carbon module. Being well in line with structure **2a**, the complex signal patterns of the carbon atoms C(2) or C(3) respectively showed coupling with C(1), C(3), and C(4) or C(1), C(2), and C(4), as illustrated in **Figure 4**. On the other hand, the lack of coupling between C(2) and C(10) or C(3) and C(10) collaborated with the singlet detected for C(10) at 117.8 ppm (**Figure 4**).

Considering all the LC-MS and ^{13}C NMR data obtained for the ^{13}C-enriched quinizolate isotopomers, it can be concluded that the quaternary carbon atom C(3) in structure **2a** is part of the intact C_5-carbon module, showing the original contiguity of the carbon skeleton of the pentose, and does not originate from the carbonyl carbon of the precursor furan-2-aldehyde. On the basis of these data, the correct structure of quinizolate is unequivocally elucidated to be the previously unreported (2*E*)-7-(2-furylmethyl)-2-(2-furylmethylidene)-3-(hydroxymethyl)-1-oxo-2,3-dihydro-1*H*-indolizinium-6-olate (**2a** in **Figure 1**).

Assignment of the ^{13}C/^{13}C correlations in the ^{13}C-enriched homoquinizolate showed major similarities in chemical shifts and $J_{C/C}$ coupling constants for the carbon atoms C(1)−C(5)

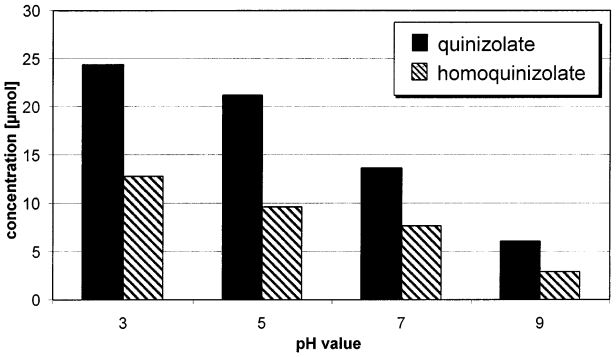

Figure 6. Influence of pH on the formation of quinizolate and homoquinizolate from xylose and L-alanine. Solutions of D-xylose (150 mmol) and L-alanine (38 mmol) in phosphate buffer (100 mL, 0.1 mol/L, pH 3, 5, 7, or 9) were heated under reflux for 3 h.

and C(6)−C(8) but strong differences in the multiplicity of C(9), as given in **Table 3**. Corresponding well with the proposed structure for homoquinizolate, the carbon C(9) showed homonuclear connectivities to C(7), C(8), and, in addition, C(9′). The hydroxymethyl group C(9′) showed the expected doublet, thus indicating that C(9′) is one of the terminal carbon atoms in the C_5-module C(6)−C(9′) derived from the original pentose backbone (**Table 3**). All these spectroscopic data obtained for homoquinizolate unequivocally revealed its chemical structure as (2*E*)-7-(2-furylmethyl)-2-(2-furylmethylidene)-3,8-bis(hydroxymethyl)-1-oxo-2,3-dihydro-1*H*-indolizinium-6-olate (**2b** in **Figure 1**), which to the best of our knowledge has not been reported previously.

Studies on the Formation Pathways. To gain further insights into the precursors involved in the formation of quinizolate and homoquinizolate, the effectiveness of several monosaccharides in generating the taste compounds was determined. To achieve this, aqueous solutions of hexoses and pentoses were thermally treated separately at pH 5.0 in the presence of L-alanine, and the amounts of both tastants produced were determined quantitatively. Both compounds were found to be exclusively formed using pentoses as the precursors; for example, 17 and 19 µmol of quinizolate and 7 and 8 µmol of homoquinizolate were produced from 150 mmol of xylose and ribose, respectively. Neither the glucose nor the fructose was able to generate the 1-oxo-1*H*,2*H*,3*H*-indolizinium-6-olates in significant amounts.

To examine the role of the amino acid moiety on tastant formation, xylose was reacted in binary mixtures with glycine, L-alanine, L-valine, L-leucine, or L-proline, and the amounts of quinizolate and homoquinizolate were determined quantitatively (**Figure 5**). The amounts of both tastants were shown to be

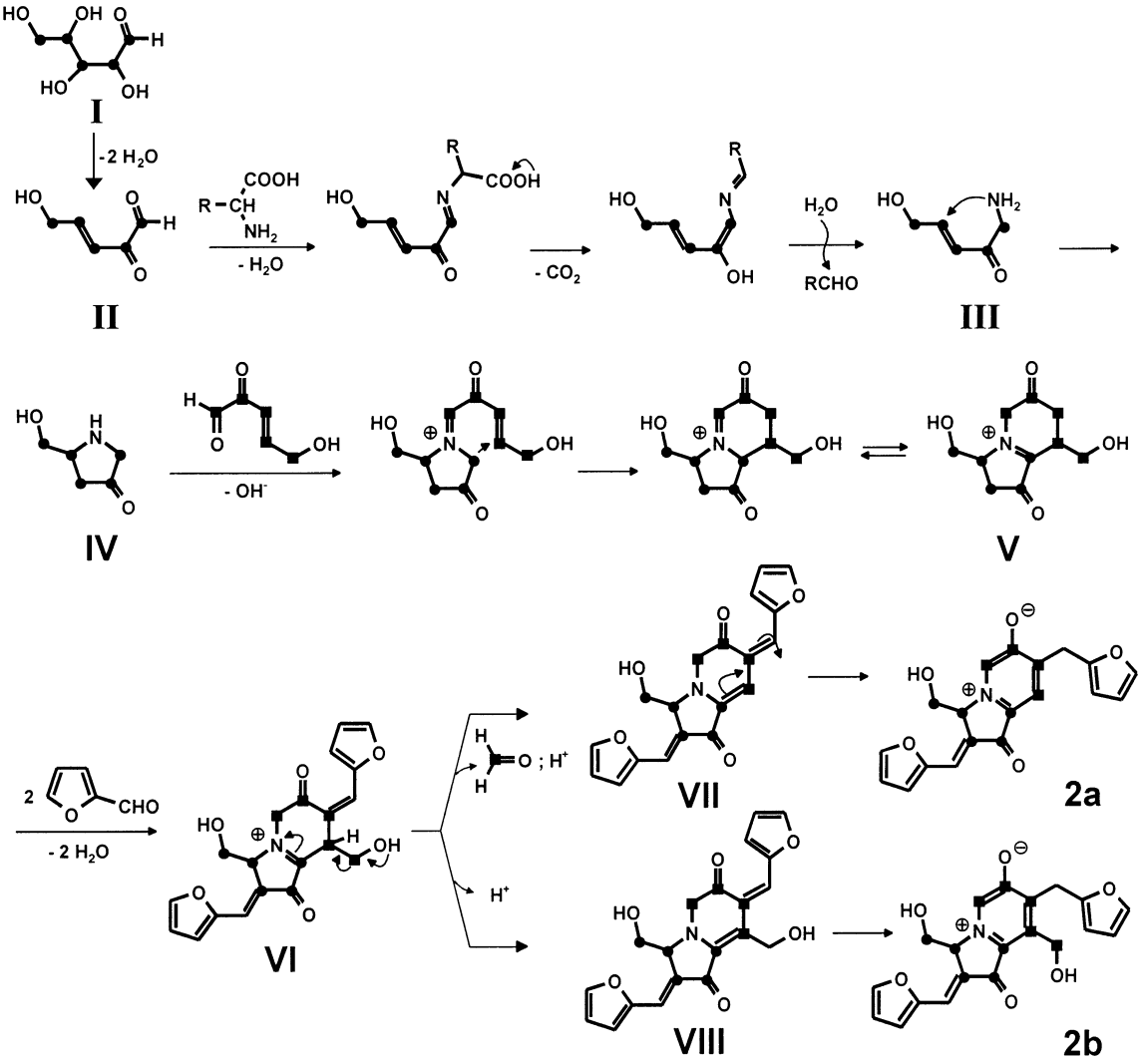

Figure 7. Proposed reaction pathway leading to the formation of the bitter-tasting quinizolate (**2a**) and homoquinizolate (**2b**) from pentoses (dots in the structures indicate ^{13}C labels; "■" and "●" differentiate ^{13}C atoms originating from different pentose molecules).

significantly influenced by the type of amino acid used; for example, both tastants were exclusively formed in the presence of any primary amino acid, whereas the secondary amino acid L-proline was ineffective as a precursor. In addition, the yields of both tastants were found to be strongly dependent on the structure of the primary amino acid used in the experiment. The highest precursor activity was found for L-valine, closely followed by that for L-leucine, generating about 3−4-fold higher amounts of quinizolate and homoquinizolate as compared to glycine and L-alanine (**Figure 5**).

To gain more detailed insights into factors governing the formation of quinizolate and homoquinizolate, the influence of the pH value on tastant formation from xylose and L-alanine was studied quantitatively (**Figure 6**). The results showed that the production of both compounds was drastically favored with decreasing pH value; for example, both tastants were formed in 4-fold higher amounts when the pH was lowered from 9.0 to 3.0.

Taking all these quantitative data into account, it can be concluded that the quinizolate and homoquinizolate are most efficiently generated when aqueous solutions of pentoses and primary amino acids are heated at low pH values. Previous quantitative studies, investigating the influence of reaction parameters on the formation of carbohydrate degradation products, clearly demonstrated that low pH values, in particular, drive the Maillard-type carbohydrate degradation reaction into the 3-deoxyosone pathway, thus leading to an accelerated formation of 3-deoxypentosulose, 3,4-dideoxypentosulose, and furan-2-aldehyde from pentoses and primary amino acids (*19*, *20*).

These observations and the findings obtained by the "bond-labeling" experiments, that the lower pyrrolinone ring in **2a** and **2b** is most likely formed from the same C_5 precursor, imply the involvement of 3-deoxypentosone-derived reaction intermediates such as 3,4-dideoxypentosone and furan-2-aldehyde in the formation of quinizolate and homoquinizolate. Assuming similar reaction pathways for both bitter tastants, the carbon fragments C(6)−C(9) and C(6)−C(9′) of the pyridinium-3-olate ring in quinizolate and homoquinizolate, respectively, were proposed to be formed from the same C_5-precursor containing the hydroxymethyl group C(9′) in homoquinizolate, and generating the C_4-carbon moiety C(6)−C(9) in quinizolate after cleavage of the hydroxymethyl group from the C_5-skeleton. On the basis of this information, the reaction pathway, illustrated in **Figure 7**, was proposed for the formation of quinizolate and homoquinizolate. Amine-assisted water elimination from the pentose (**I**) liberates the 3,4-dideoxypentosulose (**II**), a major dehydration product formed from pentoses (*20*, *21*), which upon Strecker-type reactions with primary amino acids leads to the 1-amino-5-hydroxy-3-pentene-2-one (**III**) by reductive amination. Subsequent cyclization by an intramolecular Michael-type reaction yields the 5-hydroxymethyl-3-oxo-pyrrolidine (**IV**), which undergoes further condensation with a molecule of 3,4-dideoxypentosulose (**II**), giving rise to the transient iminium ion **V**. Reaction between the two CH-acidic methylene groups in **V** and the carbonyl group of furan-2-aldehyde results in the formation of the bis-condensation product **VI**. This intermediate (**VI**) acts as a chemical switch, which has the possibility to undergo either a retro-Aldol cleavage of one molecule of formaldehyde, or a simple imine/enamine tautomerism. Retro-Aldol cleavage of formaldehyde generates the intermediate **VII**, which upon aromatization give rise to quinizolate (**2a**). As an alternative, formation of the transient enamine **VIII**, followed by aromatization, results in homoquinizolate (**2b**). The key role of the intermediate **VI** as a chemical switch in determining product formation is well in line with the finding that the ratio of quinizolate and homoquinizolate formed from pentoses is rather constant.

The LC-MS-assisted CAMOLA and the NMR-assisted bond-labeling technique presented not only offer insights into the formation pathways on a molecular level, but they are also useful to confirm the chemical structure of the target compounds and, therefore, to avoid possible pitfalls in the structure determination of complex organic molecules. Information obtained by such studies is helpful to extend the knowledge on key tastants generated by the puzzling network of Maillard-type reactions during food processing and will help to construct a route map of reactions leading to taste development in heated foodstuffs. Details obtained on the yields of potent taste compounds, their formation pathways, and their reaction intermediates might open the possibility to control and optimize the thermally induced taste development more efficiently, either by increasing the yields of sapid tastants or by inhibiting the formation of undesired compounds exhibiting, e.g., intense bitter taste.

ACKNOWLEDGMENT

We are grateful to Dr. W. Eisenreich, Institute for Organic Chemistry and Biochemistry, Technical University Munich, for measuring the ^{13}C NMR spectra, and to Mr. J. Stein for skillful technical assistance.

LITERATURE CITED

(1) Schieberle, P.; Grosch, W. Potent odorants of the wheat crumb. Differences to the crust and effect of a longer dough fermentation. *Z. Lebensm. Unters. Forsch.* **1991**, *192*, 130−135.

(2) Cerny, M.; Grosch, W. Evaluation of potent odorants in roasted beef by aroma extract dilution analysis. *Z. Lebensm. Unters. Forsch.* **1992**, *194*, 322−325.

(3) Fickert, B.; Schieberle, P. Identification of the key odorants in barley malt (caramalt) using GC/MS techniques and odour dilution analyses. *Food* **1998**, *42*, 371−375.

(4) Schieberle, P.; Pfnuer, P. In *Flavor Chemistry. Thirty Years of Progress*; Teranishi R., Wick, E. L., Hornstein, I., Eds.; Kluwer Academic/Plenum Publishers: New York, 1999; pp 147−153.

(5) Pickenhagen, W.; Dietrich, P.; Keil, N.; Polonsky, J.; Nouaille, F.; Lederer, E. Identification of the bitter principle of cacoa. *Helv. Chim. Acta* **1975**, *58*, 1078.

(6) Papst, H. M. E.; Ledl, F.; Belitz, H.-D. Bitter tasting compounds in heated mixtures of sucrose, maltose and L-proline. *Z. Lebensm. Unters. Forsch.* **1985**, *181*, 386−390 (in German).

(7) Tressl, R.; Helak, B.; Spengler, K.; Schröder, A.; Rewicki, D. Cyclo[b]azepine derivatives—novel proline-specific Maillard reaction products. *Liebigs Ann. Chem.* **1985**, 2017−2027 (in German).

(8) Shima, K.; Yamada, N.; Suzuki, E.-I.; Harada, T. Novel brothy taste modifier isolated from beef broth. *J. Agric. Food Chem.* **1998**, *46*, 1465−1468.

(9) Hofmann, T. Influence of L-cysteine on the formation of bitter-tasting aminohexose reductones from glucose and L-proline: Identification of a novel furo[2,3-b]thiazine. *J. Agric. Food Chem.* **1999**, *47*, 4763−4768.

(10) Frank, O.; Ottinger, H.; Hofmann, T. Characterization of an intense bitter-tasting 1*H*,4*H*-quinolizinium-7-olate by application of the taste dilution analysis, a novel bioassay for the screening and identification of taste-active compounds in foods. *J. Agric. Food Chem.* **2001**, *49*, 231−238.

(11) Ottinger, H.; Bareth, A.; Hofmann, T. Characterization of natural "cooling" compounds formed from glucose and L-proline in dark malt by application of taste dilution analysis. *J. Agric. Food Chem.* **2001**, *49*, 1336−1344.

(12) Frank, O.; Jezussek, M.; Hofmann, T. Identification of novel 1*H*,4*H*-quinolizinium-7-olate chromophores by application of colour dilution analysis and high-speed countercurrent chromatography on thermally browned pentose/L-alanine solutions. *Eur. Food Res. Technol.* **2001**, *213*, 1−7.

(13) Hofmann, T.; Schieberle, P. Quantitative model studies on the effectivity of different precursor systems in the formation of the intense food odorants 2-furfurylthiol and 2-methyl-3-furanthiol. *J. Agric. Food Chem.* **1998**, *46*, 235−241.

(14) Hofmann, T.; Schieberle, P. Studies on the formation and stability of the roast-flavor compound 2-acetyl-2-thiazoline. *J. Agric. Food Chem.* **1995**, *43*, 2946−2950.

(15) Hofmann, T. Characterisation of precursors and elucidation of the reaction pathway leading to a novel coloured 2*H*,7*H*,8a*H*-pyrano[2,3-*b*]pyran-3-one from pentoses by quantitative studies and application of ^{13}C-labeling experiments. *Carbohydr. Res.* **1998**, *313*, 215−224.

(16) Frank, O.; Heuberger, S.; Hofmann, T. Structure determination of a novel 3(6*H*)-pyranone chromophore and clarification of its formation from carbohydrates and primary amino acids. *J. Agric. Food Chem.* **2001**, *49*, 1595−1600.

(17) Hofmann, T. Application of site specific [^{13}C] enrichment and ^{13}C-NMR spectroscopy for the elucidation of the formation pathway leading to a red colored 1H-pyrrol-3(2*H*)-one during Maillard reaction of furan-2-carboxaldehyde and L-alanine. *J. Agric. Food Chem.* **1998**, *46*, 941−945.

(18) Bacher, A.; Rieder, Ch.; Eichinger, D.; Arigoni, D.; Fuchs, G.; Eisenreich, W. Elucidation of novel biosynthetic pathways and metabolite flux patterns by retrobiosynthetic NMR analysis. *FEMS Microbiol. Rev.* **1999**, *22*, 567−598.

(19) Hofmann, T. Quantitative studies on the role of browning precursors in the Maillard reaction of pentoses and hexoses with L-alanine. *Eur. Food Res. Technol.* **1999**, *209*, 113−121.

(20) Ledl, F.; Schleicher, E. The Maillard reaction in foods and in the human body—new results of the chemistry, biochemistry and medicine. *Angew. Chem.* **1990**, *102*, 597−734 (in German).

(21) Nedvidek, W.; Ledl, F.; Fischer, P. Detection of 5-hydroxymethyl-2-methyl-3(2*H*)-furanone and of α-dicarbonyl compounds in reaction mixtures of hexoses with different amines. *Z. Lebensm. Unters. Forsch.* **1992**, *194*, 222−228.

Received for review April 23, 2002. Revised manuscript received July 18, 2002. Accepted July 19, 2002.

JF020473K